Journal of Manufacturing Processes 60 (2020) 144–161

Contents lists available at ScienceDirect

Journal of Manufacturing Processes

journal homepage: www.elsevier.com/locate/manpro

Finish turning of hardened bearing steel using textured PcBN tools

M. Law [a,*], R. Karthik [a], S. Sharma [b], J. Ramkumar [b]

[a] Machine Tool Dynamics Laboratory, Department of Mechanical Engineering, Indian Insititute of Technology Kanpur, Kanpur, 208016, India
[b] Department of Mechanical Engineering, Indian Institute of Technology Kanpur, Kanpur, 208016, India

ARTICLE INFO

Keywords:
Hard turning
PcBN
Textured tool
Bearing steel
Laser texturing

ABSTRACT

Texturing on tools is thought to improve cutting performance by increasing tool life and reducing process forces by reducing friction between the tool and the chip, and in between the tool and the machined surface. This paper tests this hypothesis for finish turning of a hardened bearing steel using twelve differently textured PcBN tools. Of the twelve textured tools, five have textures on their rake face, three have them on the flank face below the nose, three more have textures on the flank face below the secondary cutting edge, and one has textures on the chamfer of the cutting edge. Textures of varying orientation, size, and spacing were fabricated using a laser and a focused ion beam. Cutting experiments were conducted dry at a fixed speed and feed and with chamfered low-CBN content tools. Experiments reveal that cutting performance characterized by tool life, process forces, and workpiece surface quality is relatively independent of the texture shape, size, orientation, spacing, and location. Significant crater wear was observed for cutting with all tools. Textures in the vicinity of the crater hastened wear, whereas textures away from the crater did not significantly influence cutting performance. Measured chip morphologies and their saw-tooth like characteristics were observed to be independent of texture type, as was the amount of chip adhesion on the tool's surface. Our analysis suggests that finish turning of the hardened bearing steel of interest using textured PcBN tools might not be the panacea to improving cutting performance. Though our results contribute to a nuanced understanding of how textures influence cutting performance, since our observations run contrary to expectations, further investigations are warranted to understand the role of changing cutting conditions, tool geometry, grade of the PcBN tool, and method of making the texture.

Introduction

Finish turning of components with hardness values greater than 45 HRC is as advantageous as it is difficult. Advantages include avoiding the need to grind parts, lower equipment costs, shorter setup times, and fewer process steps. These advantages have favoured the use of hard part machining in the bearing industries. However, due to bearings being made of steels with high hardness, mechanical and thermal loads are high, and machining these hard parts remains difficult. Though the use of polycrystalline cubic boron nitride (PcBN) tools with their high hot hardness and wear resistance has made possible machining of hard materials, since PcBN tools are expensive and since their wear mechanisms are complex and not completely understood yet, reliability of machining hard parts with PcBN tools remains questionable. There has hence been a lot of research over the past few decades to help realize the potential of hard part machining with PcBN tools [1–12]. This paper is also concerned with using PcBN tools to finish turn a hardened bearing steel that has hardness of 56 HRC. Our explicit aims are to understand mechanisms that limit cutting performance and to investigate solutions that may potentially improve cutting behaviour.

Past research on hard part machining with PcBN tools has focused its attention on understanding: complex wear mechanisms [1], chip formation mechanisms [2], role of binders and CBN contents [3,4], role of micro-geometry of tools [5], role of cutting parameters [6], role of variability in material properties [7], role of heat [8,9], and on developing cutting force models [9]. Comprehensive overviews of the many strides made in understanding the challenges in hard part machining with PcBN tools has been summarized nicely in the review papers by Dogra et al. [10], by Bartarya and Choudhury [11], and by Hunag et al. [12]. In general, even though previous studies help guide the design of geometries on PcBN tools, and in the selection of low CBN content tools, and in the selection of machining parameters that result in preferential saw-tooth shaped chips and improved cutting performance, recommendations to mitigate abrasive, adhesion, and other wear mechanisms to improve the tool life of these expensive PcBN tools remain elusive.

One significant method to mitigate tool wear that has gained traction

* Corresponding author.
E-mail address: mlaw@iitk.ac.in (M. Law).

https://doi.org/10.1016/j.jmapro.2020.10.051
Received 4 April 2020; Received in revised form 28 September 2020; Accepted 17 October 2020

over the last couple of decades involves a surface modification technique by fabricating textures on the rake or flank surface of the tool. Textures have been made on tools used in turning, milling, and drilling. Textures can have different geometrical shapes and sizes. Shapes can be dimples, grooves, and/or of other (ir)regular patterns. Sizes can range from nanometres to micrometres. The main mechanism that improves tool life for machining with textured tools is thought to be due to reduced contact between the tool and the chip resulting in reduced friction between the tool and the chip, which in turn helps reduce cutting forces and improve surface characteristics.

Any improvement in cutting performance with textured tools is governed by the size, the shape, and the orientation and location of the texture with respect to the cutting edge(s). For cutting of Aluminium with textured carbide tools, textures on the rake face perpendicular to the chip flow direction were found to be better than parallel textures [13]. And even though perpendicular textures were reported to be better in [13,14], others, while investigating cutting of Aluminium and steel with textured carbide tools found that textures on the rake face parallel to the cutting edge performed better [15–18], whereas, yet others found that dimpled textures performed even better [19]. Moreover, the improvements reported in [13] and in [19] with textures breaking the cutting edges run contrary to those reported in [14,16–18,20–22], in which textures were recommended to be placed away from the cutting edge, else there is a real possibility of weakening the edge and degrading tool life. Furthermore, though Koshy and Tovey [20] found that the optimal location of the textures from the cutting edge(s) was three times the feed, others observed improvements for textures placed at distances equal to or slightly greater than the feed [14–17,21,21,22]. For textures on the flank faces, Fatima and Mativenga [23], and Liu et al. [24] found that textures that are parallel to the primary cutting edge perform better than perpendicular and/or inclined textures, whereas, in [25,26], textures perpendicular to the primary cutting edge were observed to improve performance.

Potential improvements with textured tools are further influenced by the size of the texture, and by the choice of machining parameters. For example, the depth of, and pitch between textures was found inconsequential in [13,17,21]. Furthermore, in some cases, improvements were reported only for cutting at very high speeds [13], and in some other cases, forces for cutting with certain textured tools were found to increase beyond those obtained for cutting with tools without textures [13,14,17,18]. Furthermore, in other situations, the edge of the texture acts like a secondary cutting edge, and this derivative cutting action can further accelerate tool wear [27,28]. Moreover, methods of making textures are also known to influence cutting performance [22,29].

Above discussions make it clear that improvements in machining with textured tools is far from guaranteed, and indeed how texturing can sometimes degrade cutting performance instead of improving it. And despite the literature being replete with reports expounding the success of texturing in reducing forces and improving tool life in the range of ~2 – 30% [29–37], potential improvement, if any, depends on the size, the shape, the orientation, and location of the texture with respect to the cutting edge, and that all improvements are further constrained by the geometry and material of the tool, and of the workpiece being machined, and further by the choice of machining parameters, and whether cutting dry or wet.

Although a lot of research has been reported on texturing, most of it has been on texturing carbide tools for cutting of softer materials than the hardened bearing steel of interest in this paper that is to be cut with PcBN tools. In the context of using textured tools for hard part turning, there has been very limited reported work [34,38–41]. Xing et al. [38] and Orra and Choudhury [39] investigated the influence of textures filled with solid lubricants and with different geometries and orientations. Though they reported improvements in tool life for cutting with textured tools, they [38,39], as well as Kumar and Patel [34] used textured ceramic tools, and not PcBN tools that forms the focus of this paper. Furthermore, since hard turning of bearing steels is recommended to be performed in the dry condition, i.e., without lubricants [11], and since the tribological mechanisms that may improve cutting performance for textures with lubricants is very different than for the case of dry cutting with textured tools [36,42], the findings reported on hard turning using textured ceramic tools [34,38,39], though significant, are not directly relevant to the hard and dry turning of bearing steels with textured PcBN tools that this paper is concerned with. Though there is also some reported work on texturing of PcBN tools [25,26], that work concerned the machining of Inconel 718, which is relatively softer than the bearing steel of interest in this paper.

The only other work that is of direct relevance to the subject of this paper, i.e., hard and dry turning of bearing steels with textured PcBN tools was reported in [40,41]. Kim et al. [40] carried out systematic numerical finite element-based investigations to understand the role of orientation of the texture with respect to the cutting edge, the size of the texture, its distance from the cutting edge, and spacing between textures. They reported that textures farther from the edge, and with greater spacing between them, and with shallower depths result in a favourable reduction in cutting forces and friction. These studies were presumably used to guide their experimental work reported in [41]. Experiments with linear grooved textures on the rake face, made using electrical discharge machining were reported to nominally reduce forces and friction for low feed and speed cutting in comparison to cutting with tools without textures for the same cutting conditions. Seeing that cutting with textured PcBN tools may prove beneficial for hard part turning, it is the aim of this paper to present expanded and more comprehensive experimental analysis than others before us for finish dry turning of a hardened bearing steel using textured PcBN tools.

Since hard part turning of bearing steels is more of a finishing operation in which the depth of cut and feed are low, and for which there may also be as much flank contact as there is contact of the chip with the tool on the rake face, how/if textures on the flank face and/or on the rake face may prove beneficial remains unexplored, and will be addressed in this paper. Furthermore, how/if the texture's shape, size, orientation, spacing between textures as well as spacing of textures from the cutting edge(s) influence the finish turning performance of hardened bearing steels also remains unexplored, and will also be addressed in this paper. This paper will present experimental characterization of a total of twelve different texture types. These include five different texture patterns on the rake face, three each below the primary and secondary cutting edge, and one on the chamfer of the insert at exactly the theoretical tool-chip contact interface.

For textures on the rake face, influence of five different texture patterns and orientations will be discussed. Since the role of texture type and its orientation with respect to the cutting edge is yet unclear, with there being reports of perpendicular [13,14], parallel [15–18], and dimples [19] – all improving performance to varying degrees, and since no such investigation for hard turning with textured PcBN inserts exist, this paper will investigate the influence of five patterns on the rake face that include textures that are perpendicular, parallel, and aligned with the resultant cutting force direction and spaced away from the cutting edge. Furthermore, even though textures have been recommended to be placed away from the cutting edge [20], since there are reports of textures breaking the cutting edge performing well [13,19], another pattern on the rake face investigated in this paper includes that with grooves along the resultant cutting force direction but that instead break into the cutting edge. Furthermore, since there exist reports of the size of, pitch between, and spacing of the textures away from the cutting edge also affecting cutting performance to varying degrees [14,16–18,20–22], we also present experimental analysis with textures on the rake face with different groove widths and spacing between two grooves, and with different levels of spacing the textures away from the cutting edge.

Additionally, influence of three types of textures each on the flank face below the secondary cutting edge and on the flank face below the nose will also be discussed. Since the role of texture orientation on the flank surfaces is also not clear, with there being reports of parallel [23,

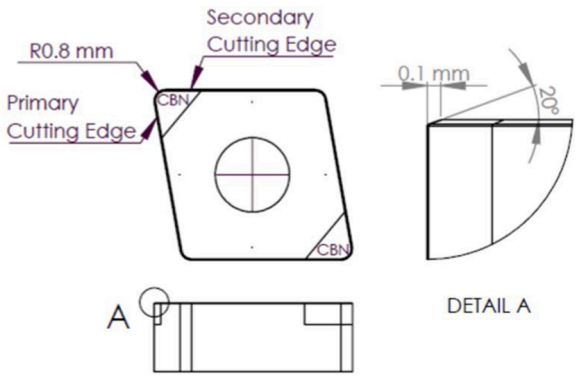

Fig. 1. Geometric details of the PcBN tool.

24] and perpendicular [25,26] texture types both faring well, and since no such analysis for hard turning using textured PcBN tools exists, this paper will also investigate the role of textures on the flank faces that include dimples, and grooves that are perpendicular and parallel to the rake face.

This experimental plan detailed in the next section of the paper is more comprehensive than most other previously reported work on texturing. Furthermore, for reliability, each experiment is repeated at least three times. A total of 60 experiments were hence conducted. This number includes cutting with tools without textures.

The remainder of the paper is organized as follows. At first, the tool and workpiece specifications are discussed. We then discuss fabrication and geometrical characterization of textures. The section that follows discusses the experimental setup to measure forces, surface characteristics of the machined workpiece and to monitor tool wear. Measured tool wear characteristics, and chip morphologies along with measured force and workpiece surface characteristics are then discussed for the case of cutting with tools without textures, followed by comparative analysis of cutting with all textured tools. Discussions are followed by a summary and the main conclusions of the paper.

Tool and the workpiece specifications

This section describes the tool geometry, tool material properties, and workpiece material specifications.

The PcBN tool

Since tools with low CBN contents and negative geometries are preferred for hard machining applications [10–12], a tool with low CBN content, i.e., one that had ~45% CBN, and a titanium-based binder was used in these investigations. CNGA 120408S-01020-L1-B CBN010 inserts [43] were selected, and their geometry is as shown in Fig. 1. As is evident from Fig. 1, the insert has a chamfer of 0.1 mm × −20 °. The edge radii are 15 μm ± 5 μm. This insert was mounted on a DCLNR2525M12-M type holder [43], which had a rake angle of −6 °, and an inclination angle of −6 °. Hence, the effective rake angle was −26 °.

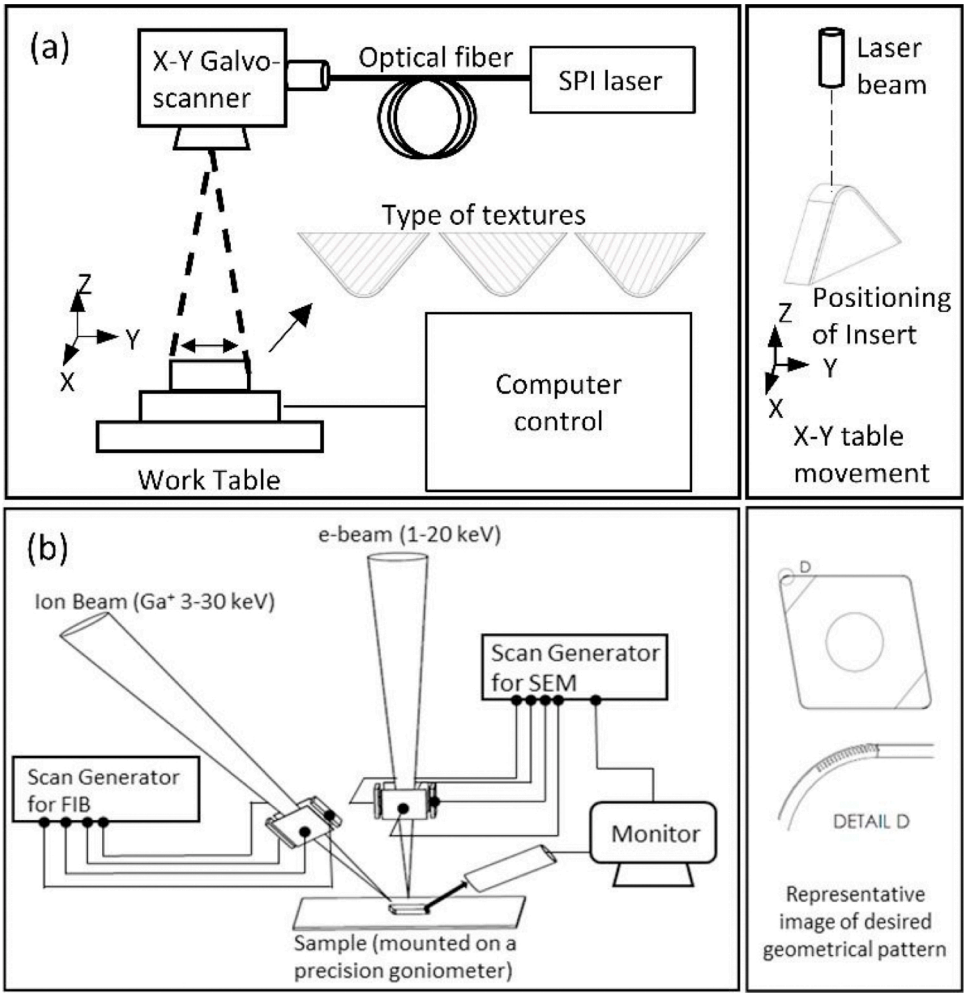

Fig. 2. Schematic showing methods to fabricate textures. (a) The laser texturing setup, (b) the setup for focused ion beam milling.

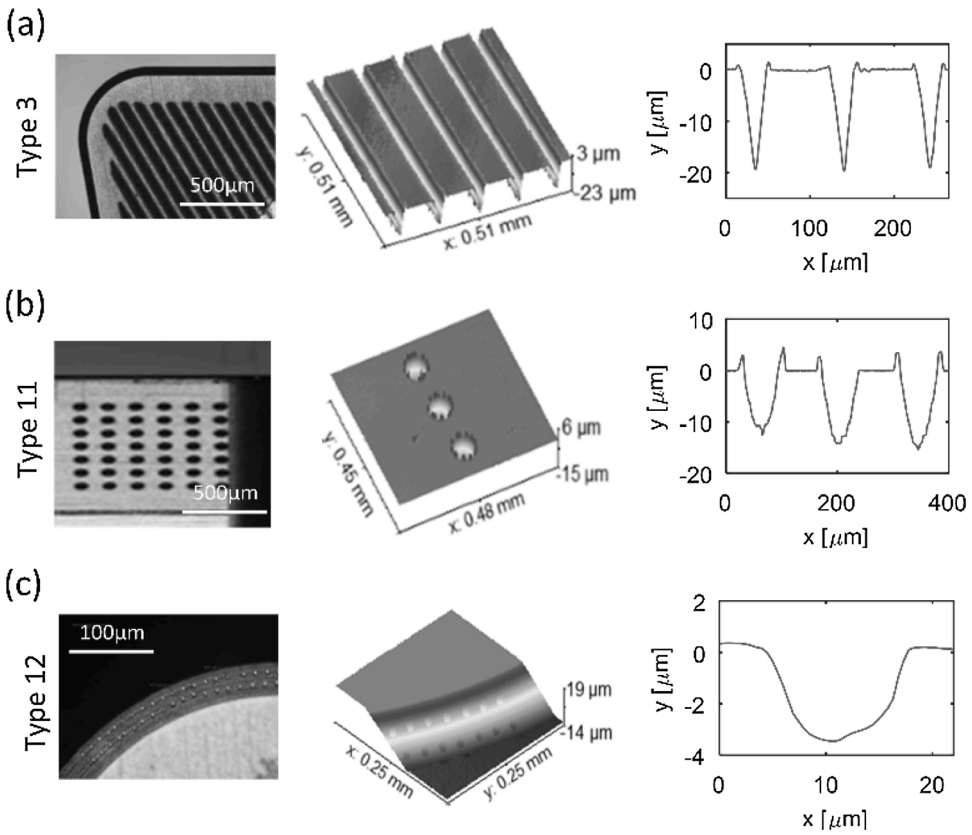

Fig. 3. Geometrical features of three representative textured tools. (a) Textures on the rake face made along the direction of the resultant cutting force, (b) dimples on the flank surface below the secondary cutting edge, and (c) dimples on the chamfer.

The workpiece

The bearing steel used in these investigations had a composition of 0.96% C, 1.55% Cr, 0.33% Mn, 0.16% Si, by weight, with the remainder being Fe. A tubular workpiece with an outer diameter of ~115 mm, and a wall thickness of ~25 mm was used since it was easier to through harden and temper. Measured hardness of the workpiece along the thickness direction was observed to be 56 HRC ± 3 HRC. The variability in hardness is within the ± 5% hardness tolerance as per the ISO 3685 standard [44].

Fabrication and geometrical assessment of different texture patterns

This section first discusses the procedure to fabricate textures, which is followed by discussions on the measured geometry of the fabricated textures.

Fabricating the textures

Unlike others before us that fabricated textures on PcBN tools using the electric discharge machining method [41] or by using femtosecond lasers [26], we prefer to use an easy to use fibre laser for all but one texture type which has much smaller features than what is easily possible to make using the fibre laser. For the texture pattern with small features we use the focused ion beam milling method.

For laser texturing, we use a SPI-SP-200C fibre laser system operating at a 1070 nm wavelength with a maximum power of 200 W. The laser beam profile was Gaussian. A galvo-scanner system with f-theta lens having a focal length of 160 mm was used to focus the laser beam on the substrate. Inserts were placed on a three-axis numerically controlled stage as shown in the schematic of the setup in Fig. 2(a). Though the continuous wave laser beam can be modulated to generate a pulsed beam of durations between 0.1 µs to 90 ms with a repetition rate range of 1 Hz to 100 kHz, we settled on using a pulse width of 5 µs with repetition rates of 15 kHz and scanning speeds of 6 m/min. These parameters were observed to result in preferential material removal by melt expulsion [45] and reduced re-solidified edges [45]. Furthermore, because of the thermal nature of material removal, the desired groove depth was found to depend on the laser power and the number of pulses per spot (or on the number of passes in some cases), and the groove width was found to depend on the laser power and the pulse width. The depth and width were hence confounded. Hence, laser parameter selection was also done to meet the desired geometrical specifications of the texture. To place textures away from the cutting edge(s), a specially designed aluminium mask was placed on the tool. All textures made on the rake and flank surfaces of the tool were made using this laser-based process. The feature size, i.e., the width and depth of textures made with the laser ranged from 35 to 60 µm, and 10–25 µm, respectively.

For making dimples on the chamfer with smaller features, we used the focused ion beam milling method. This was necessary since the chamfer is small (~100 µm) and controlling the dimple size to be within ~15 µm and to place the textures within ~15 µm from the edges was beyond the scope of the SPI laser due to factors such as diffraction limited focused spot size, thermal interaction and re-solidified burr. The setup to make dimples on the chamfer using a FEI-make Nova Nano Lab 600 focused ion beam milling equipment is shown schematically in Fig. 2(b). As was done for the case of laser texturing, the parameters for focused ion beam milling were also arrived at such as to ensure that the desired geometrical features of the texture were met. The parallel milling mode [46] of operation was preferred with a voltage of 30 kV, a current 7 nA, and a dwell time 1 µs.

All tools were ultrasonically cleaned in ethanol before and after texturing. Furthermore, all textured tools were analysed in an electron

Table 1
Geometric features and specifications of the twelve different texture patterns being investigated.

Texture on	Texture type			Mean spacing between textures [μm]	Mean width/ diameter of texture [μm]	Mean depth of texture [μm]	Mean distance from the primary/secondary cutting edge [μm]	Representative image
Rake face	Grooves ∥ to the primary cutting edge	1	a	70	35	10	200	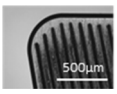
			b	100	35	10	200	
			c	70	50	20	100	
			d	100	50	20	100	
	Grooves ⊥ to the primary cutting edge	2	a	70	35	10	200	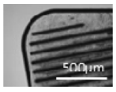
			b	100	35	10	200	
			c	70	50	20	100	
			d	100	50	20	100	
	Grooves along the resultant cutting force direction	3		150	50	25	350	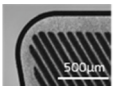
	Grooves along the resultant cutting force direction, but breaking the edge	4		70	35	10	–	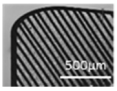
	Dimples along the resultant cutting force direction	5		150	60	15	250	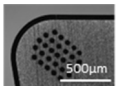
	Grooves ∥ to the rake face	6		150	50	25	210	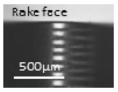
Flank face below nose radius	Grooves ⊥ to the rake face	7		150	50	25	230	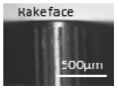
	Dimples	8		170	55	15	210	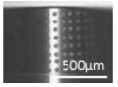
	Grooves ∥ to the rake face	9		150	50	25	200	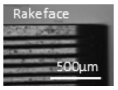
Secondary flank face	Grooves ⊥ to the rake face	10		150	50	25	230	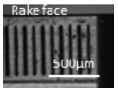
	Dimples	11		150	60	15	265	
Chamfer	Dimples	12		30	15	5	15	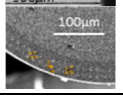

probe micro analyser and the results were contrasted with tools without textures to ensure that texturing does not change the composition of the Boron, Nitrogen, and the Titanium binder.

Geometrical assessment of textured tools

Textured patterns were observed under an optical microscope and the geometric features were extracted using measurements done on a NanoMap-D-make optical profilometer. Three representative textures, one with grooves on the rake face made along the direction of the resultant cutting force, another with dimples on the flank surface below the secondary cutting edge, and another with dimples on the chamfer, along with their measured geometrical features are shown in Fig. 3. Preliminary experiments for cutting with a tool without textures were used to estimate the in-plane resultant cutting force, and grooves were then made along the direction of the resultant cutting force.

As is evident from Fig. 3, geometric features, i.e., the size, spacing between textures, and spacing of textures from the cutting edge(s) are consistent. Also evident for the textures made with the laser (Fig. 3(a–b)) is that though there exists a re-solidified burr due to the melt expulsion phenomena, the height of the burr is not observed to be greater than ~3 μm. Since this is negligible in comparison to the feature size, it is not expected to play any significant role. Tapering of the grooves and the dimples is characteristic of laser and focused ion beam milling fabrication methods and is difficult to avoid [29]. Similar geometric characterization was carried out for all textured inserts, and the results are summarized in Table 1.

Table 1 shows images of all the twelve textured inserts and lists their geometrical features. Of the twelve texture types shown in Table 1, five textures, i.e., texture types 1–5 concern texture patterns made on the rake face. Texture types 6–8 concern patterns made on the flank face below the nose radius, and texture types 9–11 concern patterns made on the flank face below the secondary cutting edge. Texture type 12 concerns dimples made on the chamfer of the insert at exactly the theoretical tool-chip contact interface.

The five patterns on the rake face include grooves that are parallel (type 1), perpendicular (type 2), and aligned with the resultant cutting force direction and spaced away from the cutting edge (type 3), and another texture pattern with grooves along the resultant cutting force direction but that instead break into the cutting edge (type 4). Rake face patterns also include dimples placed away from the cutting edge (type 5). Texture type 1(a–d) and type 2(a–d) include textures on the rake face

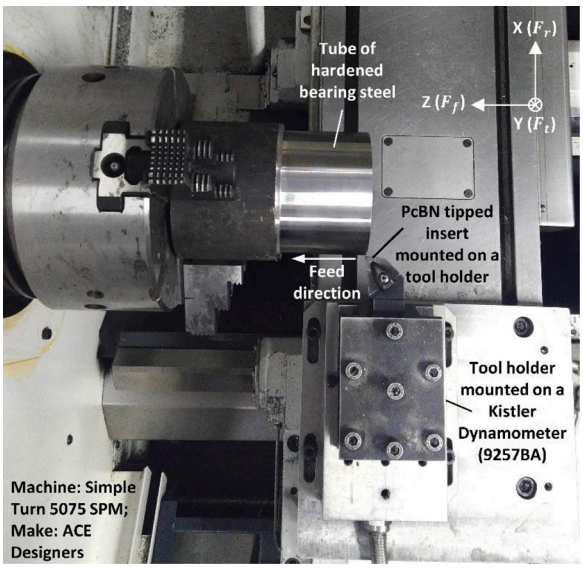

Fig. 4. Experimental setup showing the workpiece mounted in a three-jaw chuck on a CNC turning machine along with tool mounted on a force dynamometer.

with different levels of spacings between textures and different levels of spacing textures away from the cutting edge(s). Texture types 1 and 2 also include textures with different groove widths and depths. Since the method of making textures with the SPI laser confounds the width and depth, any increase in the width of the texture is accompanied by a corresponding increase in the depth of the texture. To investigate if textures on the flank surfaces below the nose and the secondary edge play any role in reducing the contact and friction between the tool and the machined workpiece surface, types 6–8 and types 9–11 include dimples, and grooves that are perpendicular and parallel to the rake face, respectively. Features, spacing, placement, and orientation of textures listed in Table 1 were decided based on recommendations in [13–26,29].

Experimental setup and characterization procedures

All machining experiments were done on the setup as shown in Fig. 4. A rigid ACE-make SimpleTurn5075 machine with a spindle power of 7.5 kW was used. The workpiece was clamped in a hydraulically controlled three-jaw chuck. The overhang from the chuck was consistently kept at ~100 mm. All experiments were conducted at a cutting speed of 170 m/min and with a feed of 0.2 mm/rev. The depth of cut was kept consistent at 0.2 mm. These cutting parameters were selected based on the tool manufacturers' recommendation. Prior to initiating measurements, the outer skin of the workpiece layer was machined away at a very low speed and feed using a regular tungsten carbide tool.

To assess machining performance with different textured tools, we measured forces during cutting, and monitored tool wear and measured surface characteristics at predetermined intervals of cut. We also monitored and characterized chip and tool wear morphologies using a JEOL-make JSM – 6010LA scanning electron microscope (SEM).

Since the depth of cut is of the order of feed, and both are less than the nose radius, and since the primary wear mechanism observed was a crater on the rake face near the secondary cutting edge, and not flank wear (more on this is discussed in Section 5), the usual stopping criterion for such analysis, i.e., the time/length of cut at which the primary flank wear reaches a value of ~300 μm – as suggested by the ISO 3685 standard [44] is not directly applicable herein, and the stopping criteria for all experiments is instead taken to be the length of cut until when the inserts chips. Furthermore, since we are cutting tubes, and not bars, to eliminate any potential vibrations due to cutting tubes when the wall thickness reduces considerably, tubes were cut till the wall thickness of the tubes reduced to the half its original value.

Forces were measured using an instrumented and dynamically calibrated Kistler-make dynamometer (9257BA) – shown in Fig. 4. All three components of forces, i.e., the tangential F_t, radial F_r, and feed F_f forces were measured at intervals of every 210 mm of cut length. Cutting force data was acquired using the MALDAQ module within the CutPRO® software [47].

Surface characteristics of the machined workpiece were measured using a MITUTOYO-make Surftest SJ-210 portable surface roughness tester. For every measurement of the workpiece surface characteristics, three different locations on the surface, each 120° apart were measured and averaged for one data point. The machined workpiece surface was cleaned with acetone before measuring its characteristics. We measured and recorded R_a, R_q, R_z, and RS_m. Like in the case of force measurements, workpiece surface measurements were also made at intervals of every 210 mm of cut length.

Wear analysis was performed under a NIKON-make Eclipse LV100 optical microscope. The insert was removed from the tool holder, handled carefully, and placed under the optical microscope for analysis, and then returned to the machine for cutting. Unlike force and surface measurements which were made at intervals of every 210 mm length of cut, since wear measurements require the experiment to be stopped and for the insert to be removed, these measurements were more involved, and hence these measurements were made at intervals of every 420 mm of cut length.

Cutting performance of tools without textures

The cutting performance of tools without textures is characterized by the wear observed on the tool, the progression of measured forces, and the evolution of measured surface characteristics. Representative chip and tool morphologies obtained from the SEM characterization are also discussed. These results serve as benchmarks against which the cutting performance of the twelve textured tools is assessed.

Progression of tool wear

The progression of wear is summarized in Fig. 5, which shows images of a representative insert without textures measured at different lengths of cut (LOC). The insert for which results are shown below, chipped at a length of cut of 1680 mm. As is evident from Fig. 5, the primary flank wear is insignificant, reaching at most ~40 μm when the insert chips. The dominant mode of wear is a crater wear on the nose near the secondary cutting edge. The crater was observed to form within a cut length of 70 mm, and the size of the crater was observed to grow with increasing time/lengths of cut. This is not entirely unusual. Similar wear behaviour for cutting with PcBN tools has been reported by others too [6,41].

SEM and EDX characterization

SEM characterization was carried out on the rake face of untextured inserts before and after cutting. These results are summarized in Fig. 6 which includes images of the rake face of the tool that has markers where the elements were identified using EDX analysis. Fig. 6 also lists the averaged weight percentage of the main elements identified at the different marker locations. The main elements of interest shown in the insets in Fig. 6 include Boron (B), Nitrogen (N), Titanium (Ti), and Iron (Fe), if/when present. Other major elements that were identified and are classified under the 'Others' category include Carbon (C) and Oxygen (O), and minimal quantities of Strontium (Sr) and Tungsten (W).

As is evident from Fig. 6, for the virgin insert, there is no Fe detected, and the CBN content at 45.1% confirms that this is indeed a low-CBN content tool. As is also evident, EDX analysis after cutting for a length of 70 mm confirms that there is major adhesion of the chip on the tool –

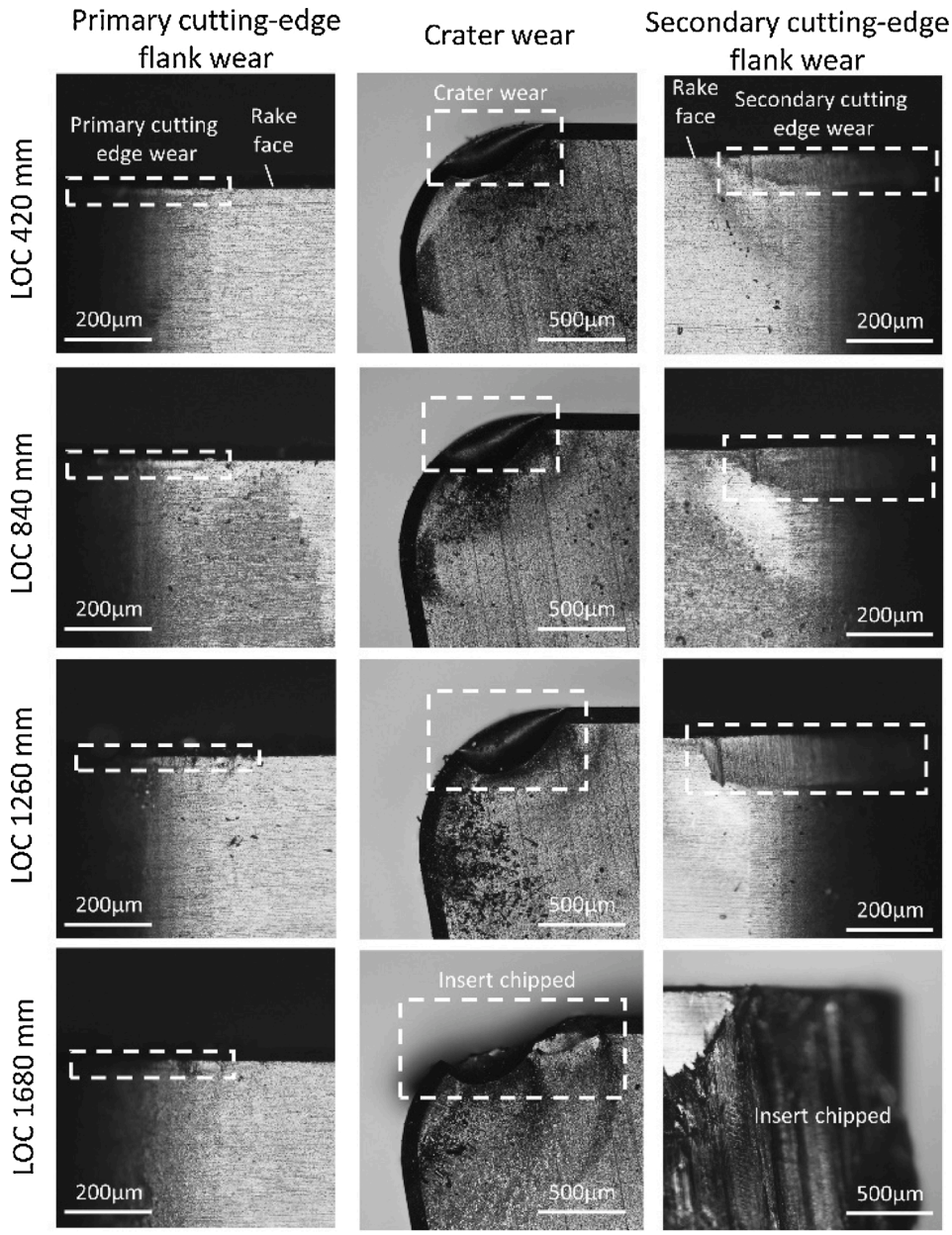

Fig. 5. Typical wear progression characteristics for cutting with tools without textures. Regions of wear are highlighted in all images.

evident from the high percentage of Fe detected. Fe is detected within the crater and on the rake face even ~1 mm away from the cutting edge. SEM images after cut lengths of 420 mm and 840 mm show the gradual progression of the crater wear, and EDX analysis at these cut lengths indicate increased adhesion of Fe from within the chip taking place on the rake face. Wear being dominated by adhesion is like what was reported in [41]. Since elements reported in Fig. 6 are averaged over several locations shown by the markers on the SEM images, the low Boron and Nitrogen content detected for worn inserts could be due to the chip adhesion on the surface that clouds the detection of these elements. Furthermore, since this analysis confirms that there is a lot of adhesion of the chip on the rake face, ability of the planned textures on the rake face to reduce contact between the chip and the tool to reduce adhesion is warranted.

Measured chip morphologies

To understand the evolution of chip morphology with increasing lengths of cut for cutting with tools without textures, SEM characterization of chips was performed for chips collected after certain predetermined cut lengths were reached. Representative results for chips measured only along the thickness direction are summarized in Fig. 7 for cut lengths of 70 mm and 840 mm, respectively. The bottom of these chips was in contact with the rake face of the tool. The saw-tooth characteristics of the chip are governed by the nature of thermoplastic instabilities in the primary shear zone [2] and due to cyclic crack initiation and propagation [48]. As is evident from Fig. 7, as the cut length increases, the pitch of the saw-tooth like profile, as well as the height of the saw-tooth reduces. Since an increase in the size of the crater with increasing lengths of cut is associated with a change in the cutting-edge characteristics due to wear, and since chip curl and morphology are also governed by cutting-edge characteristics evolving due to tool wear [2,48–51], the observed changes in the chip's morphology, we conjecture, can be attributed to the change in the cutting-edge characteristics due to wear. How/if cutting with textured inserts potentially influences chip morphology is discussed later.

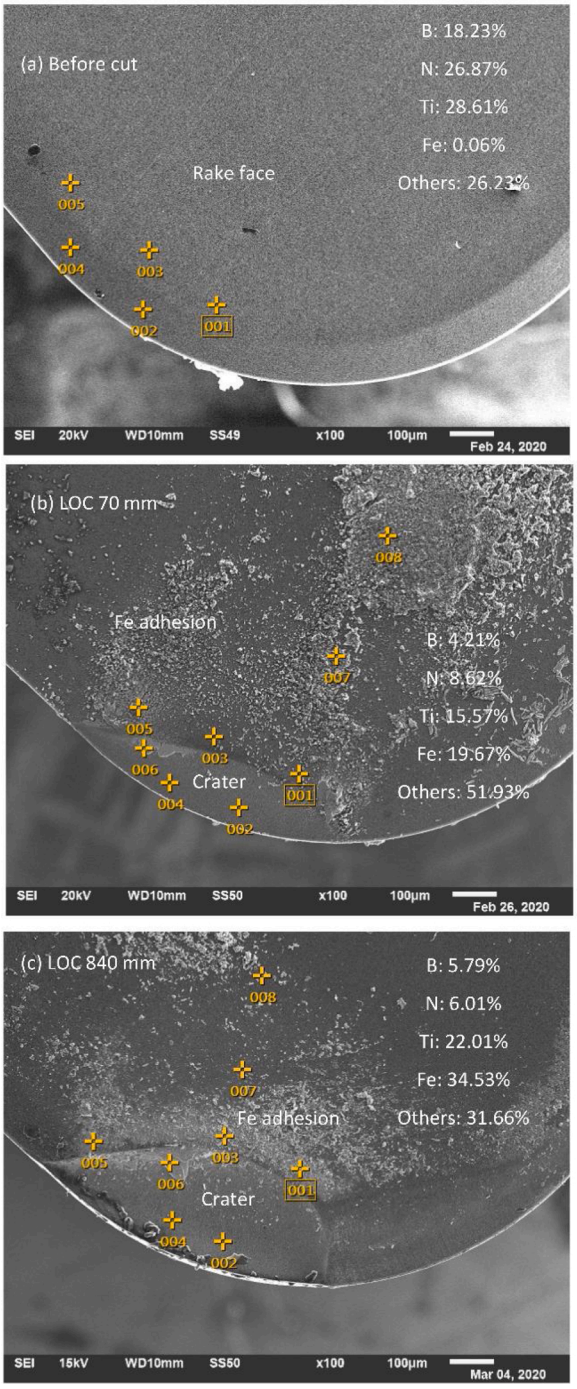

Fig. 6. SEM and EDX characterization of the rake face of a representative cutting tool without textures to show chip adhesion and crater evolution at different lengths of cut (LOC). (a) before cutting, (b) LOC of 70 mm, and (c) LOC of 840 mm.

Measured force characteristics

Measured force components changing with time/length of cut are shown in Fig. 8, which also includes in an inset the force components for the initial 70 mm of the length of cut. Since the depth of cut is of the order of the feed, and since both these are less than the nose radius, the radial component of the force is comparable to the tangential force – as is evident from Fig. 8. As is also evident, all force components increase from the cut length of 70 mm to the cut length of 420 mm, and then remain almost constant until a length of cut of 1260 mm. Since the insert

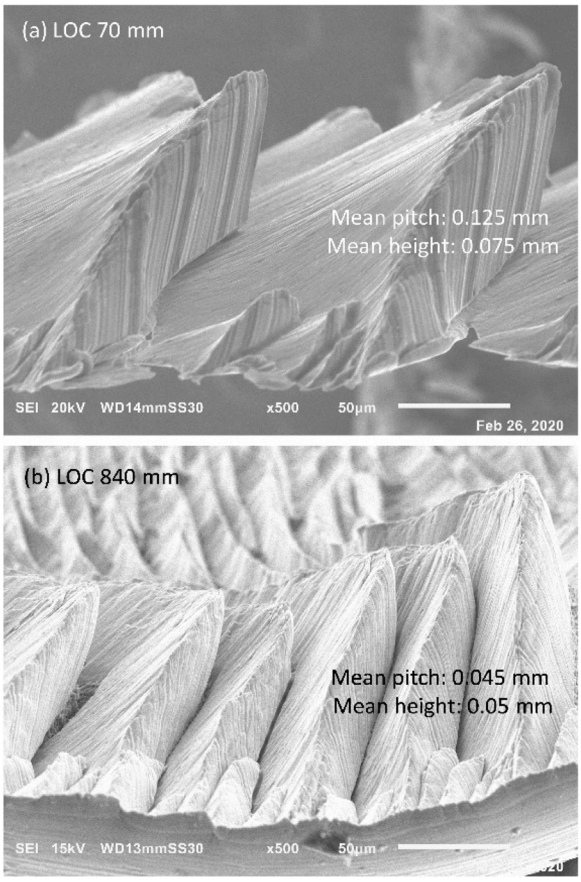

Fig. 7. Morphology of chips in their thickness direction for cutting with a representative cutting tool without textures. Results are shown for different lengths of cut (LOC). (a) LOC of 70 mm, and (b) LOC of 840 mm.

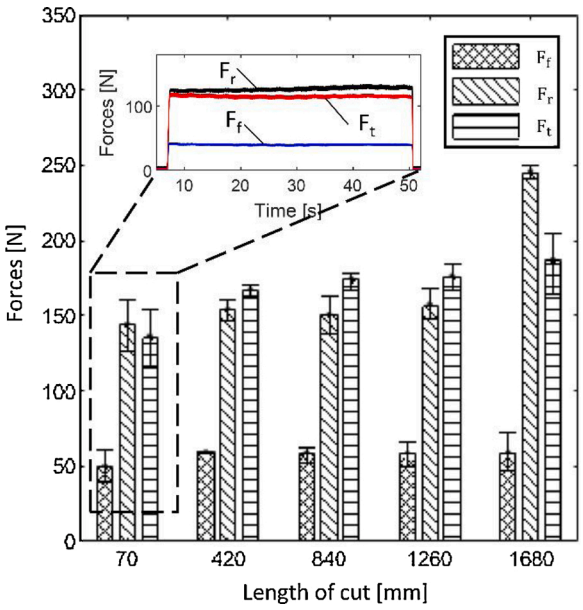

Fig. 8. Measured force characteristics and their evolution with increasing lengths of cut for cutting with untextured inserts.

for which results are reported in Fig. 8 chipped at a length of cut of 1680 mm, a sudden increase in the radial force component is observable. These observations suggest that force components do not increase

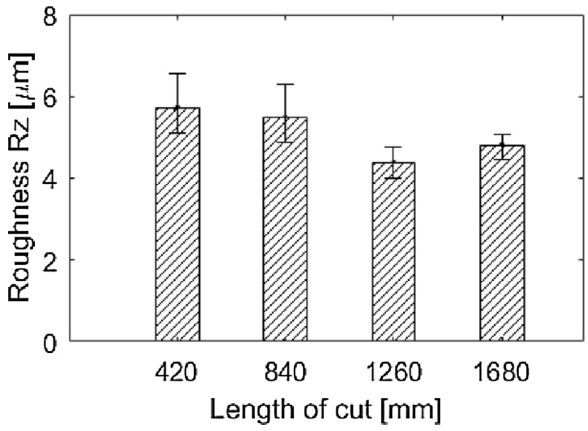

Fig. 9. Progression of measured workpiece surface characteristics for cutting with inserts without textures.

significantly as the cutting length increases unless the insert chips. These observations are like what were reported in [1]. Since all experiments were repeated at least three times, Fig. 8 also shows the lowest and highest observations (refer the whiskers in Fig. 8), along with the mean, and as is evident, if the outliers due to sudden increase in forces due to chipping are neglected, force measurements were observed to be repeatable within ~4% for all experiments conducted for cutting with tools without textures.

Measured workpiece surface characteristics

Measured workpiece surface characteristics are shown in Fig. 9. Even though we measured R_a, R_q, R_z, and RS_m, Fig. 9 only reports how R_z changes with increasing lengths of cut. Since R_z is a measure of averaged peaks and valleys over the sampled lengths, and since any extremities in the peaks and/or valleys will influence the final R_z value more than they might in the measure of R_a, if the shape of the cutting edge was to change due to wear on the flank surfaces, R_z would capture that change in the measured workpiece surface characteristics. However, as is evident from Fig. 9, R_z remains consistently around ~5.5 μm ± 1 μm for all lengths of cut until the inserts chip. The variations observed in R_z in Fig. 9 correspond to the lowest and highest observations made across measurements that were repeated at least three times.

The flank wear for cutting with untextured tools remains insignificant. The flank wear reaches at most ~40 μm on the primary cutting edge, and at most ~120 μm on the secondary cutting edge before the insert chips – see Fig. 5. Since the flank wear is low, it does not degrade surface roughness of the machined surface reported in Fig. 9. These observations are consistent with those reported elsewhere in [1,52,53]. Furthermore, though there is an increase in the crater wear with increasing lengths of cut, since the crater is not in direct contact with the machined surface, the crater wear does not directly influence the workpiece surface characteristics, and hence R_z remaining consistent as the length of cut increases is understandable.

Having systematically characterized the cutting performance with inserts without textures, and having observed material transfer from the chip to the tool – suggesting adhesion, and having seen that this adhesion causes more crater wear than wear on the primary and/or secondary flank surfaces, and since the ISO 3685 standard does not make any recommendations to determine the tool life based on wear on the secondary flank, or based on the depth of the crater, the stopping criteria for comparative analysis of any potential influence of textures on the cutting performance is taken to be the length of cut until the insert chips. Furthermore, since EDX analysis suggests that there is a change in the elements on the rake face with increasing lengths of cut, and since chip morphologies are also observed to evolve with increasing lengths of cut, these too are taken to be metrics to investigate the influence of textures.

Although force and surface characteristics were observed to not change significantly with increasing lengths of cut, cutting performance characterized by these for the case of cutting with textured inserts are still compared with the results for the case of cutting with inserts without textures.

Comparative analysis of cutting performance of all twelve textured tools

This section presents comparative analysis of the cutting performance with all twelve textured tools and benchmarks those results with the results for cutting with tools without textures. At first, we present the tool wear characteristics of all tools, followed by EDX analysis and chip morphologies for representative textured tools to help explain the observed wear behaviour. This is followed by results for the achieved length of cut until the inserts chip for all tools, which in turn is followed by comparative analysis of the measured force and workpiece surface characteristics for cutting with all tools.

Comparative analysis of progression of tool wear

Progression of tool wear for all twelve insert types is summarized in Fig. 10. Although tool wear was monitored on the rake face and on the primary and secondary flanks, since the crater wear dominates, Fig. 10 only shows images for the crater wear for textures on the rake face, and for textures on the flank surfaces, images for the rake and the primary and/or the secondary flank surfaces are also shown. Moreover, even though tool wear for all tools was monitored at intervals of completing 420 mm of lengths of cut, Fig. 10 reports results for cutting with texture types 1–11 for lengths of cut of 420 mm, 840 mm, and finally the condition when the insert chips, whereas for the case of cutting with the insert with texture type 12, wear is shown at a length of cut of 140 mm, 420 mm, and when the insert chips. Since every experiment was repeated three times, Fig. 10 shows representative images from experiments with one tool for every type of texture. For texture types 1 and 2, i.e., for grooves on the rake face, Fig. 10 reports results of type 1(c) and type 2(c) only, and the influence of varying feature size and spacing is discussed subsequently.

As is evident from the comparisons in Fig. 10, differences in crater wear patterns for cutting with all textured tools is minimal, and this observation is consistent with reports in [41]. Furthermore, it is also stark that chipping of the insert always occurs due to the growth of the crater that weakens the secondary cutting edge. Moreover, as is evident from results for cutting with tools with textures on the rake face (see results for texture type 1, 3 and 5), if/when the crater grows large enough to reach the texture, the crater eats into the textures, and may even contribute to hastening the catastrophic failure of the insert through chipping. It is also further evident from results for cutting with type 2 textures, that if the texture is far enough from the cutting edge, it plays no significant role in potentially reducing the tool-chip contact. For cutting with textures with grooves on the rake face made in the direction of the resultant cutting force, but that break the cutting edge, i.e., for cutting with type 4 inserts, the textures breaking the cutting edge further weaken the edge and result in premature catastrophic chipping.

For cutting with tools with texture types 6–11, i.e., for textures on the flank below the nose radius and on the flank surface below the secondary cutting edge, the dominant wear mechanism remains that of the crater wear. Moreover, as is observed for craters eating into the textures on the rake face, on the flank surfaces too, if/when the crater reaches the textures, local weakening of the insert is observed, which in turn may accelerate chipping of the tool. Furthermore, if/when the textures are far enough away from the crater frontier, the textures potentially play no role in reducing the tool-workpiece contact.

For cutting with the case of textures made on the chamfer on the 'exact' tool-workpiece contact location, i.e., for cutting with type 12 textured tools, the crater forms early, and beings to 'wash' away the

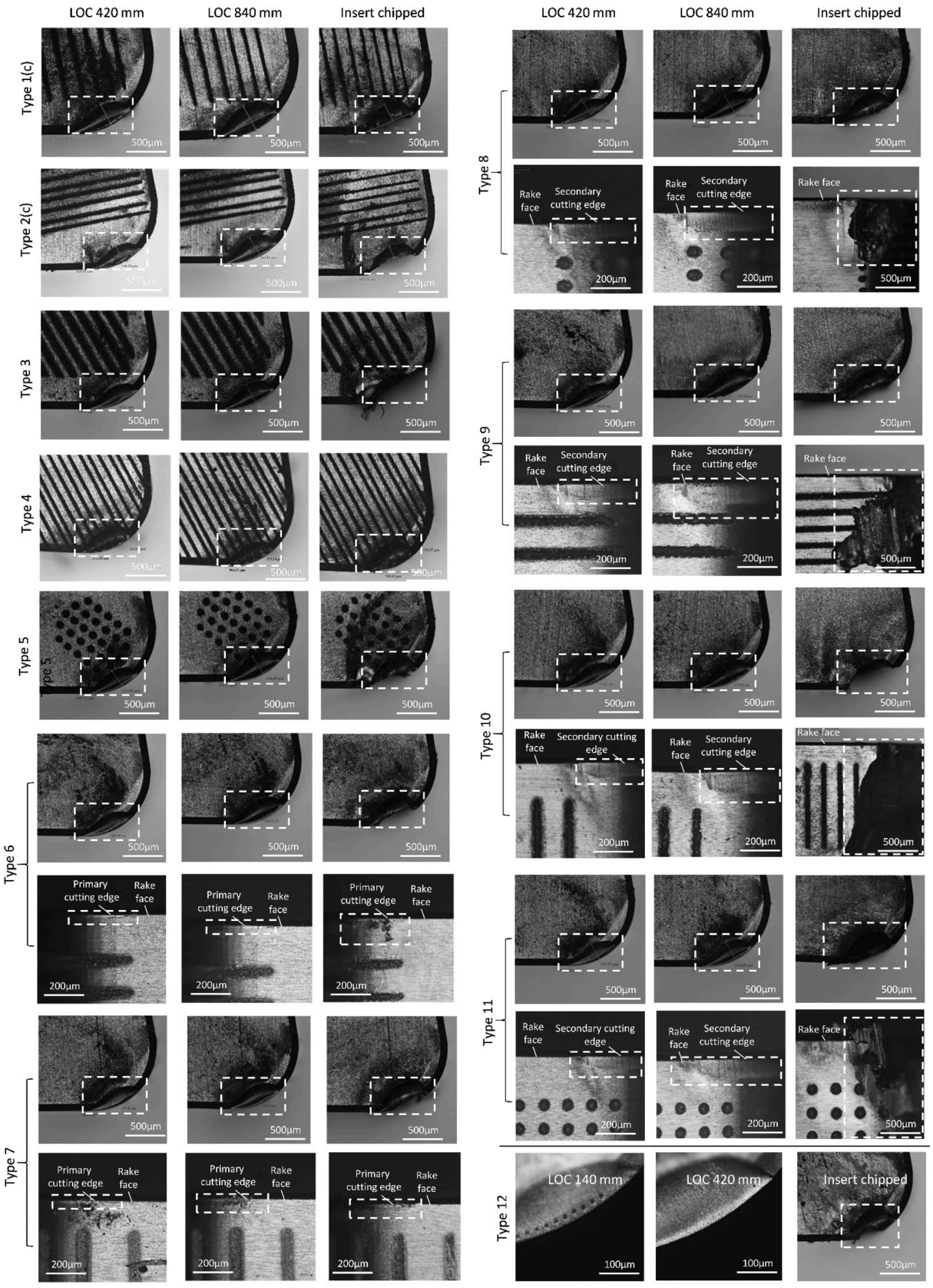

Fig. 10. Typical wear progression characteristics for cutting with all twelve textured tools. Regions of wear are highlighted in all images.

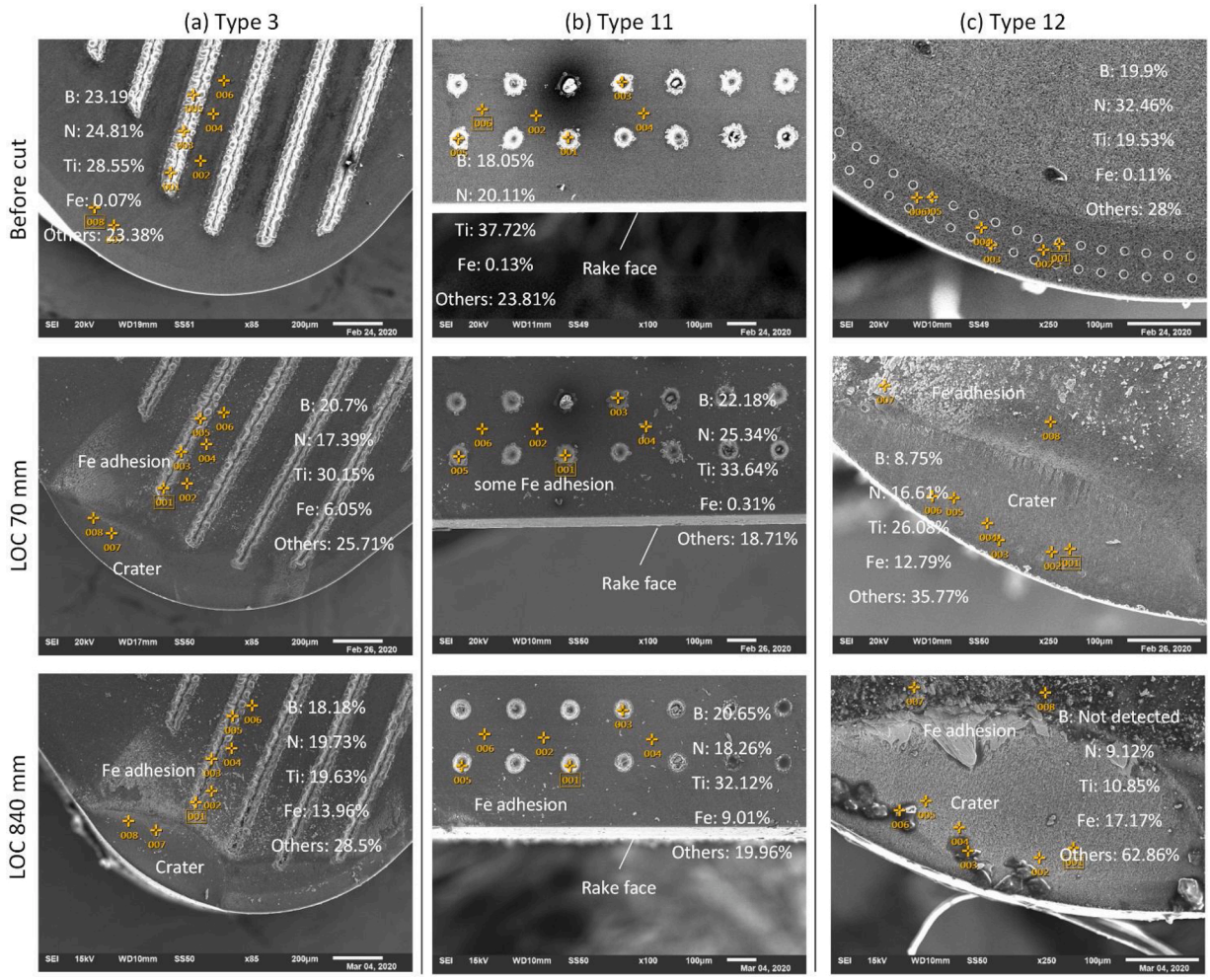

Fig. 11. SEM and EDX characterization of the rake and flank face for cutting with inserts with three representative texture types to show chip adhesion and crater evolution at different lengths of cut. (a) Results for texture type 3, (b) results for texture type 11, and (c) results for texture type 12.

textures. Hence, any potential benefit of reduced contact between the tool and the chip because of these textures is lost early in the process. Once the dimples on the chamfer are washed away, which happen before reaching a length of cut of 420 mm, the insert behaves like an untextured tool for the remainder of its life until the crater grows significantly and causes chipping of the tool.

Having presented the wear characteristics for all twelve textured tools, and having observed that the crater wear characteristics are the same for textured tools as they are for cutting with tools without textures, wear mechanisms are confirmed with EDX analysis of three representative textured tools as discussed next.

Comparative analysis of EDX characterization results

As was done for the case of cutting with tools without textures, since cutting with tools with textures is also limited by craters being formed, to investigate if there is as much adhesion of the chip on the tool in the presence of textures, EDX characterization was again carried out for textured inserts and results of three representative textured patterns are summarized in Fig. 11. The three patterns for which results are shown in Fig. 11 are the same as those shown in Fig. 3, i.e., for textures on the rake face made along the direction of the resultant cutting force (type 3), dimples on the flank below the secondary cutting edge (type 11), and for dimples on the chamfer (type 12). Again, as was shown for the case of cutting with tools without textures, Fig. 11 also lists the averaged weight percentage of the main elements (B, N, Ti, and Fe) identified at the different marker locations – also shown on SEM images in Fig. 11. And, as before, i.e., as was shown for the case of cutting with tools without textures, and as was shown above in the discussions on the progression of wear characteristics, SEM and EDX analysis results are shown before cutting, and at representative cut lengths of 70 mm and 840 mm, respectively.

As is evident from Fig. 11, the CBN content for all textured tools before cutting ranges from ~40 – 50% with there being negligible amount of Fe being detected. However, as is also evident from Fig. 11, for the case of the textured tool with grooves on the rake face, as the length of cut increases, the amount of Fe detected also increases. This again suggests that there is significant amount of adhesion of the chip on the rake face. Elemental analysis on the secondary flank surface suggests that there is less amount of adhesion of the workpiece material on this surface than on the rake face. Elemental analysis on the dimpled region on the chamfer suggests that there is also a significant amount of adhesion of the chip on the surface – evident from the high percentage of Fe detected. At a cut length of 840 mm, for the case of textures on the chamfer (type 12), there also appears a significant amount of Carbon (52.78% within the 'Others') – suggesting that the surface is also charred. Also evident from the SEM images in Fig. 11 is the increase in the size of the crater with an increase in the length of cut. These observations suggest that even with textured tools, there is as much adhesion of the chip on the tool as is there is for the case of cutting with tools without textures, and that there is no significant difference in the characteristic features of the crater in comparison to the case of cutting with tools

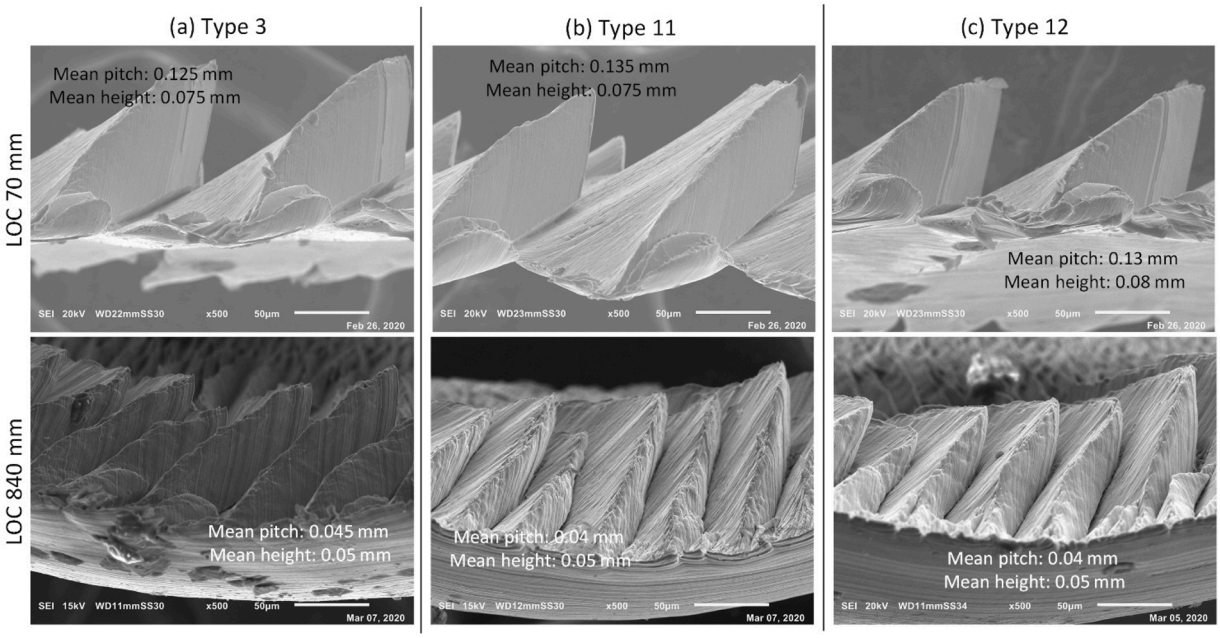

Fig. 12. Comparative analysis of morphology of chips at different lengths of cut for three representative textured tools. (a) Results for texture type 3, (b) results for texture type 11, and (c) results for texture type 12.

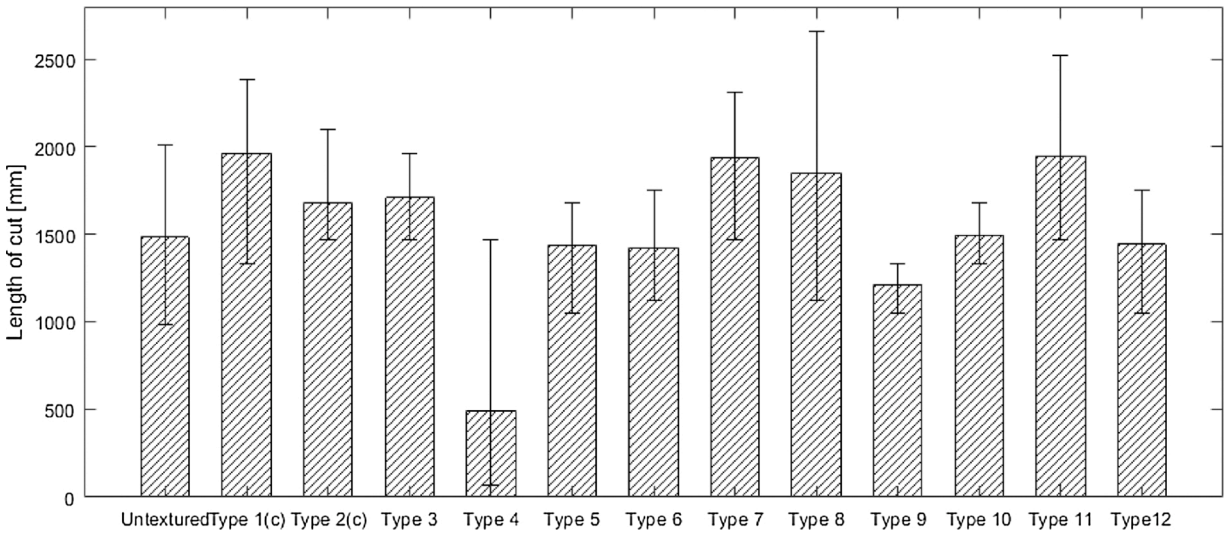

Fig. 13. Comparative analysis for length of cut for cutting with all tools, textured, or not, until all inserts chip. For classification of texture types, please refer to Table 1.

without textures.

Comparative analysis of measured chip morphologies

To understand how morphologies of the chips for the case of cutting with textured tools are potentially different than for the case of cutting with tools without textures, and to understand how chip morphology evolves with increasing lengths of cut, SEM characterization of chips was carried out for cutting with three representative textured tools, and the results are summarized in Fig. 12. The tools for which results are shown in Fig. 12 are the same as those for which EDX characterization was presented above in Fig. 11. Though chips were collected and measured at cut intervals of 70 mm, 420 mm, and 840 mm respectively, results reported in Fig. 12 are only for cut lengths of 70 mm and 840 mm, respectively.

As is evident from Fig. 12, the morphology of the chips for cutting with textured tools retain their saw-tooth like character. It is also evident from Fig. 12 that as the length of cut increases, the mean pitch and height of the saw-teeth reduce with increased lengths of cut for cutting with all three types of textures. This is consistent with observed behaviour for cutting with tools without textures and is also consistent with earlier reported results [41]. Moreover, there appear no significant difference in the saw-teeth characteristics for cutting with different textured tools. These observations suggest that cutting with textured tools does not appear to change the nature of deformation and/or the chip morphology in comparison to cutting with tools without textures.

Comparative analysis of length of cut until inserts chip

Comparative analysis for lengths of cut until all inserts, textured, or not, chip is summarized in Fig. 13 and Fig. 14. For texture types 1 and 2, i.e., for grooves on the rake face, Fig. 13 reports results of type 1(c) and

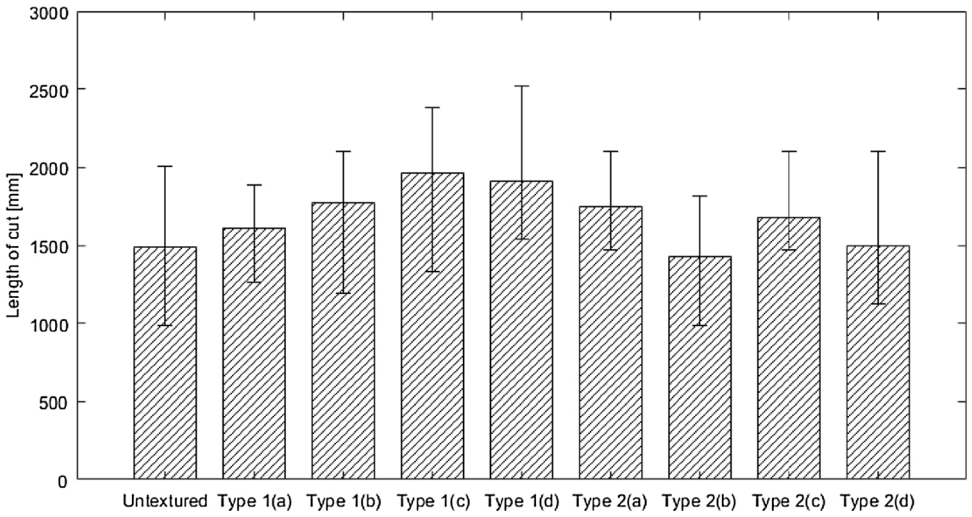

Fig. 14. Comparative analysis of the length of cut until inserts chip for textures on the rake face (types 1(a-d), and 2(a-d)) with different feature sizes and spacing characteristics. For classification of texture types, please refer to Table 1.

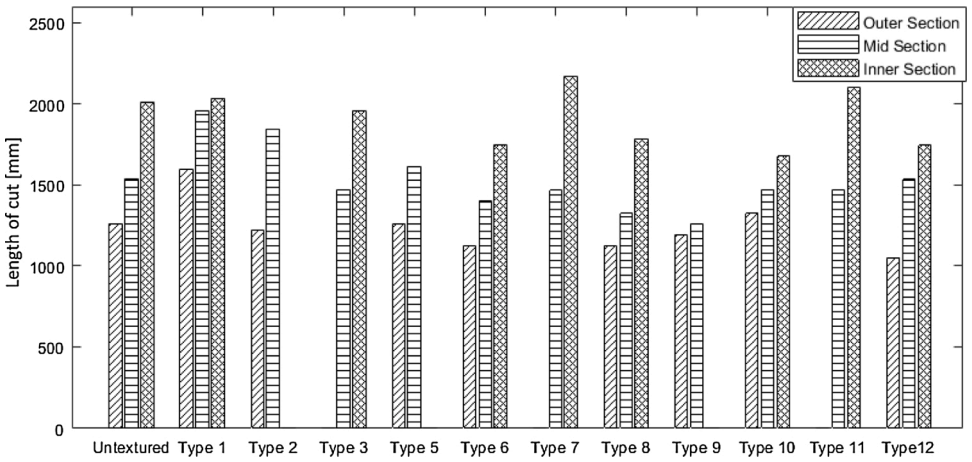

Fig. 15. Comparative analysis of the length of cut until inserts chip for experiments conducted at different diametrical sections. For classification of texture types, please refer to Table 1.

type 2(c) along with results for all other ten types of textures, and the influence of varying rake face texture feature size and spacing is shown in Fig. 14.

As is evident from Fig. 13 and Fig. 14, of the 12 different texture types investigated, our analysis suggests that the mean length of cut when the inserts chip (which is a proxy for tool life) for cutting with texture types 1, 2, 3, 7, 8, and 11 is up to ~30% greater than cutting with an insert with no textures. Our analysis also suggests that cutting with texture types 5, 6, 9, 10, and 12 results in an up to ~20% reduction in the mean length of cut, whereas for cutting with texture type 4, there is a ~66% reduction in the mean length of cut till the inserts chip. Since cutting with textured tools in which the texture breaks the cutting edge (s) results in premature catastrophic failure, the length of cut until the inserts chip for those tools (texture type 4) is significantly less than the length of cut for cutting with all other tools, textured, or not – as is evident from Fig. 13. These observations are consistent with those reported in [14–18,20–22], which suggest placing the texture away from the cutting edge.

From the comparisons of mean lengths in Fig. 13, it may be tempting to concluded that cutting with texture types 1, 2, 3, 7, and 8 is indeed beneficial to improve tool life, whereas cutting with texture types 4–6, 8, 9, 10, and 12 is detrimental. However, if variations for the lengths of cut when the different textured inserts chip is accounted for, it is evident that the lowest and/or the highest observation for the different textured inserts is no different than the mean length of cut for cutting with the insert without textures.

The large variations in the lengths of cut until the inserts chip observed in Fig. 13 and in Fig. 14 can be explained as follows. If the tube can be imagined to be partitioned into three sections such that the outer section represents the case when cutting begins when the diameter of the tube is ~113 mm, and continues until the tube diameter reaches ~107 mm, and cutting in the mid-section begins when the diameter of the tube is ~106 – 107 mm, and continues until the tube diameter reaches ~97 mm, and cutting in the inner section begins when the diameter of the tube is ~96 – 97 mm, and continues until the tube diameter reaches ~86 mm, then it can be inferred that when experiments are performed for cutting in the inner section, the length of cut until when the insert chips was observed to be consistently higher than the length of cut for cutting in the mid and the outer sections respectively.

These observations are summarized in Fig. 15, and suggest that the mean length of cut until the insert chips for cutting in the outer section is ~1216 mm, for cutting in the middle section, it is ~1530 mm, and for cutting in the inner section it is ~1915 mm. This suggests that if, where the experiment was conducted, i.e., at which section, is not controlled for, it may lead one to wrongly conclude that cutting with some inserts with some textured patterns may lead to an increased length of cut

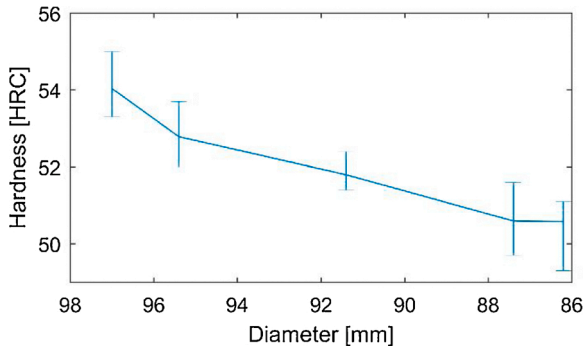

Fig. 16. Measured surface hardness characteristics changing with a change in the dimeter of the tube(s).

before chipping. The dependence of the achievable length of cut until the insert chips on the diametrical section being cut explains the large variations observed in Fig. 13 and in Fig. 14.

Even though experiments for every texture pattern were repeated at least three times each, not all experiments for each texture type were conducted at all diametrical sections. Hence, data for some texture types for some diametrical sections is not available and is hence missing in Fig. 15. Fig. 15 also does not report results for cutting with textures that break the edge. Results in Fig. 15 for the case of cutting with tools with texture types 1 and 2 at different diametrical sections are averaged over their sub-types, i.e., the lengths of cut until the inserts chipped for cutting with tools with textures on the rake face with different feature sizes and spacing characteristics were averaged for cutting with them over different diametrical sections. And only the mean achievable length of cut for every diametrical section is shown in Fig. 15. All twelve experiments (four sub-types being repeated three times each) for cutting with type 2 textured tools were conducted for cutting only at the outer and the mid sections of the tube, and hence data for cutting at the inner diametrical sections is also not available.

Furthermore, if lengths of cut until inserts chip are to be compared for cutting at similar diametrical sections, it may again be tempting to conclude that cutting at the inner diametrical section with texture type 7 results in an ~8% improvement in tool life, and cutting with texture type 11 results in a ~4.5% improvement in tool life. However, if cutting with the same textured insert types 7 and 11 were to be compared for cutting at the middle section, it is evident that there would be a ~4.5% reduction in the life of the tool. Since most results in Fig. 15 correspond to only a single data point, and since cutting at different sections results in different results, observations are not conclusive.

The phenomena of cutting at the inner sections resulting in a greater length of cut until the inserts chip, we postulate, is related to cutting process induced softening. Softening is known to occur due to heat retention in the workpiece which makes the workpiece softer and potentially easier to cut [54,55]. Since it is difficult to measure temperature during cutting, we instead measured the surface hardness to monitor how it changes with different diametrical sections. We treat the measured surface hardness characteristics as a proxy for any temperature related influences. In situ hardness was measured using a portable TIME-make hardness testing device. Results for hardness measured at different diameters is shown in Fig. 16 – which presents results only for the representative case of cutting with tools without textures.

As is evident from Fig. 16, the hardness changes from ~54 HRC for cutting at the mid-section to ~49 HRC for cutting at the inner section. Since measurements were repeated and averaged at every section, the variation in measured mean values shown in Fig. 16 correspond to lowest and highest observations. Seeing that the hardness of the tube is lesser at the inner section than at the mid-section and/or the outer section, and since softer materials are easier to cut, if cutting at different sections of the tube is controlled for, then it is unsurprising that cutting

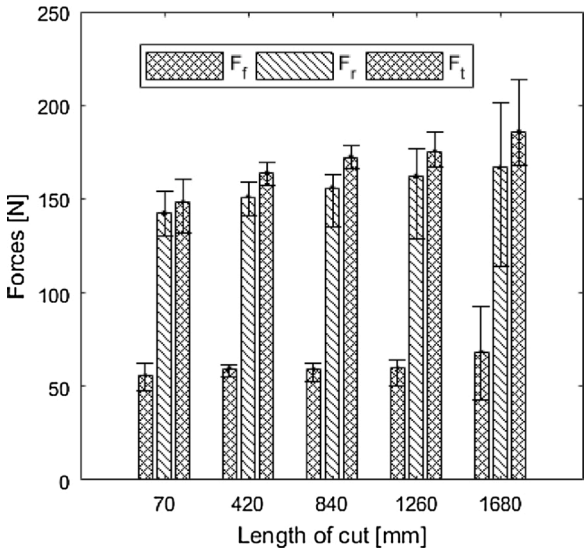

Fig. 17. Progression of measured force characteristics with an increase in the length of cut for cutting with a textured tool with dimples on flank surface below the nose radius.

with some textured inserts that cut the tube at the inner section chipped later than for cutting with tools, textured, or not, at the mid and outer diametrical sections.

Comparative analysis of measured force characteristics

At first, to establish how/if force characteristics for cutting with textured tools evolve differently over the length of cut as compared to cutting with tools without textures, for a representative case of cutting with an insert with dimples on the flank surface below the nose (type 8), measured force characteristics are shown in Fig. 17. The variation in forces correspond to the lowest and highest observations made across measurements being repeated at least three times. And as is evident, even though the measured force characteristics appear to increase slightly with increasing lengths of cut, the rate of increase is insignificant. This is consistent with the observations for the force characteristics for cutting with tools without textures – see Fig. 8.

Though Fig. 17 shows the measured averaged forces for cutting with a single textured insert, similar behaviour was observed for cutting with all other textured inserts, and hence force components were averaged over their length of cut to enable a comparative analysis of the force behaviour for cutting with all twelve textured tools. These comparisons are shown in Fig. 18 and are limited to only comparing the main tangential force component. Furthermore, for the linear groove type textures on the rake face, results in Fig. 18 are shown only for texture type 1(c) and for texture type 2(c), along with forces for all other texture types, except for the case of cutting with textures that break the edge. As is evident from Fig. 18, comparisons of forces with and without textures shows that there is no significant change in force components for cutting with textured inserts. Furthermore, there is no discernible change in the force component between different textured tools.

Though Fig. 18 only reports results of force characteristics for cutting with linear grooves on the rake face with tool type 1(c) and type 2(c), force analysis for type 1(a–d), and for type 2(a–d), shown in Fig. 19, also suggests that forces do not change over their length of cut, and nor are the force magnitudes very different than results shown in Fig. 18. The variation in forces observed in Fig. 18 and in Fig. 19 for each texture type are due to forces being low during the first pass, and due to forces being high during the pass in which the inserts chip. These variations can also be understood from the results shown in Fig. 17. These observations are different than those reported in [40], in which the size of the

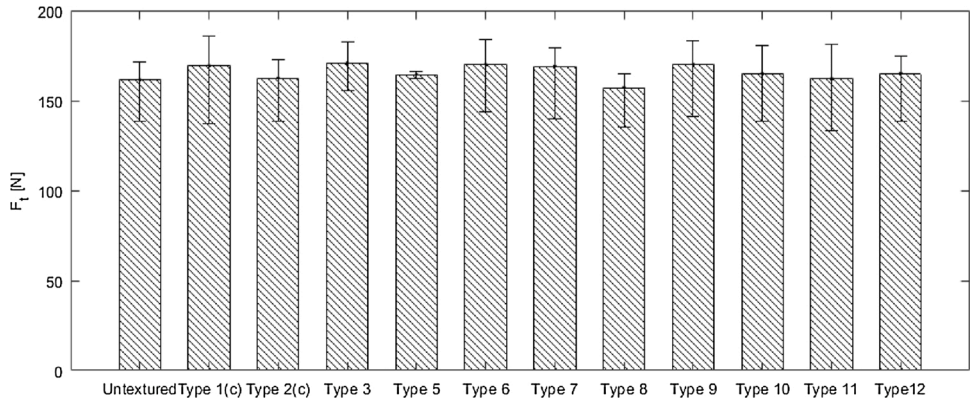

Fig. 18. Comparative tangential force characteristics for cutting with all textured inserts. For classification of texture types, please refer to Table 1.

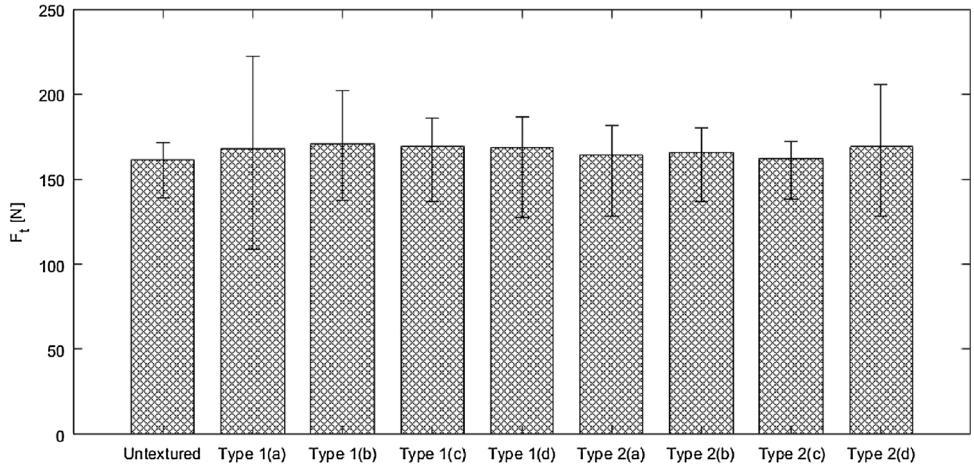

Fig. 19. Comparative tangential force analysis for textures on the rake face with different feature sizes and spacing characteristics. For classification of texture types, please refer to Table 1.

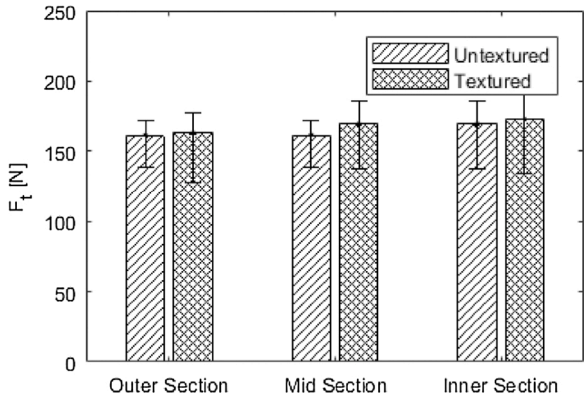

Fig. 20. Measured tangential force component for cutting at different diametrical sections. Results are shown for cutting with tools without textures, and for a representative case of cutting with tools with a texture type 1(c).

texture and its placement from the cutting edge was reported to influence cutting forces. However, that analysis and those conclusions were based on numerical finite element simulations [40], and no experimental proof was offered. Furthermore, though Fig. 18 and Fig. 19 only reports results for the main tangential force, similar behaviour was observed for the feed and radial components.

Since analysis for the achievable lengths of cut before inserts chip suggested a strong dependence on the diametrical section being cut, if thermal softening is indeed taking place, as is indeed confirmed by the hardness reducing with a reduction in the diameter of the tube, this should also manifest in a reduction in the cutting forces for cutting in the inner section. However, the comparative analysis of the representative tangential force component shown in Fig. 20 for cutting with tools with and without textures shows that forces do not exhibit a reducing trend for cutting at the inner section. The results in Fig. 20 for the textured tool

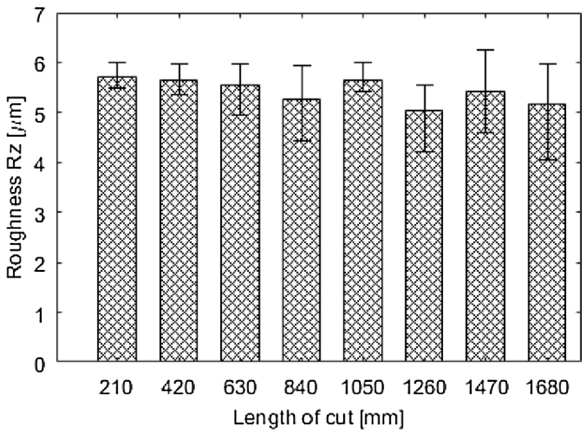

Fig. 21. Progression of measured surface characteristics with an increase in the length of cut for cutting with a textured tool with dimples on flank surface below the nose radius.

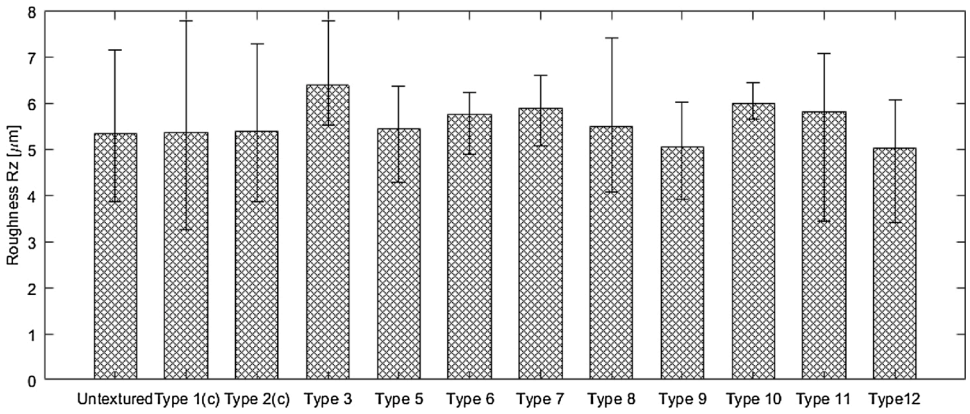

Fig. 22. Comparative analysis for measured surface roughness for all textured inserts. For classification of texture types, please refer to Table 1.

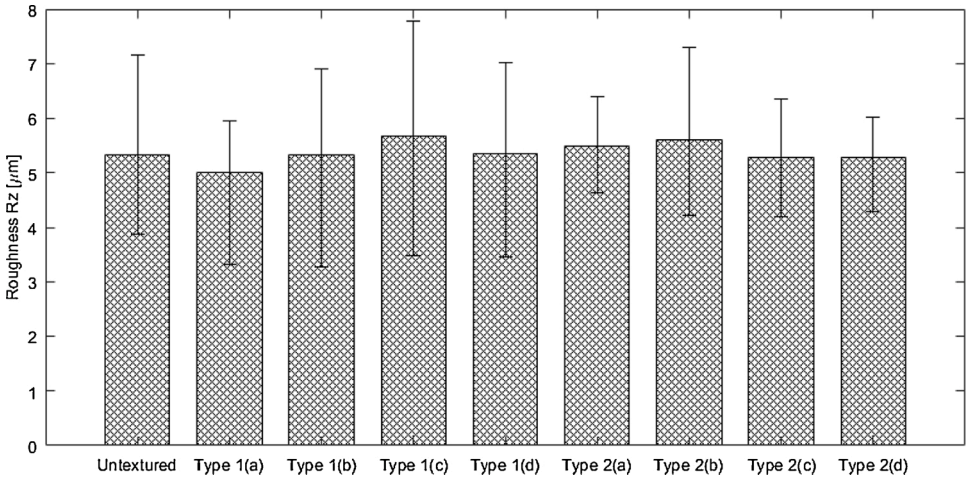

Fig. 23. Comparative measured surface characteristics for textures on the rake face with different feature sizes and spacing characteristics. For classification of texture types, please refer to Table 1.

are for the case of cutting with a tool with textures on the rake face, i.e. texture type 1(c). The whiskers in Fig. 20 correspond to the variations in the measurements, i.e., to the lowest and highest observations. Since observations in Fig. 20 show that the forces do not vary much with cutting at different sections, and even though there is some thermal softening taking place that results in a higher length of cut until the insert chips for cutting at the inner sections than cutting at the middle and outer sections, that thermal softening does not manifest itself into a reduction of process forces for cutting at the inner sections. This oddity cannot be completely explained yet.

Comparative analysis of measured workpiece surface characteristics

Influence of textures on the machined workpiece surface characteristics changing with the length of cut are presented herein. As a representative example of how R_z changes with time (length of cut) for cutting with a textured tool, the case of a textured tool with dimples on the flank surface below the nose is considered (type 8). Results are shown in Fig. 21, and as is evident R_z remains consistently around ~5.5 μm ± 1 μm, which is of the same order as that for cutting with tools without textures. Since R_z is governed by the flank wear, and since the flank wear remains low and uniform, reaching at most ~40 μm on the primary cutting edge, and at most ~120 μm on the secondary cutting edge before the insert chips – see Fig. 10, these low levels of flank wear do not adversely influence the surface finish as the length of cut increases – and this remains consistent with observations for cutting with tools without textures, and with observations reported elsewhere in [1, 52,53].

Though the results in Fig. 21 are limited to characterizing how surface characteristics change with the length of the cut for one representative textured tool, similar observations were made for cutting with all textured tools. The surface characteristics were hence averaged over the length of cut for all tools, and the resulting characteristics are compared with each other in Fig. 22. Results of workpiece surface characteristics in Fig. 22 are shown only for texture type 1(c), and texture type 2(c), along with surface characteristics for all other texture types, except for the case of cutting with textures that break the edge. And, measured surface characteristics for all other type 1(a–d) and type 2(a–d) are shown in Fig. 23. As is evident from Fig. 22 and Fig. 23, the mean value for R_z for all experiments, i.e., textured, or not, ranges from between 5 μm–6 μm, with some outliers. The outliers (variations) in the measured R_z for results shown in Fig. 21 – 23 correspond to the lowest and highest observations in the measurement(s). These observations (from Fig. 22 and Fig. 23) suggests that the mean surface roughness does not vary much with different texture types.

Conclusions

Finish turning of a hardened bearing steel using twelve differently textured low-CBN content tools was characterized at fixed cutting conditions. The aim was to establish how texture size, shape, orientation, spacing, and location influence the cutting performance – something that remained unaddressed until now. Cutting performance was characterized by wear, tool life, chip morphologies, and measured process

forces and workpiece surface characteristics.

Cutting performance was found to be relatively independent of the texture shape, texture orientation, of texture size, of texture spacing, and of texture location. Significant crater wear was observed for cutting with all tools, textured, or not. Textures in the vicinity of the crater hastened wear, whereas textures away from the crater, played no role. Measured chip morphologies and their saw-tooth like characteristics were observed to be independent of texture type, as was the amount of chip adhesion on the tool's surface. Cutting induced softening of the workpiece observed in its thickness direction made cutting at the inner sections of the tube easier and resulted in greater tool life. If cutting at different diametrical sections of the tube is controlled for, no significant differences in tool life was observed for cutting with all inserts – textured, or not.

Though our analysis suggests that texturing does not significantly improve the finish turning performance of the hardened bearing steel of interest, and as such, even though our observations run contrary to our own expectations, and to many reports that purport and expound texturing to be the panacea to improve cutting performance, our analysis contributes to a nuanced understanding of hard turning using textured PcBN tools and helps establish the boundaries of knowledge.

Since our investigations were limited to dry cutting of bearing steel with fixed cutting parameters, and with a chamfered low-CBN content tool, how/if a change in cutting parameters, or a change in the edge geometry, or a change in the CBN content of the tools, and/or a change in the method of making textures can potentially influence and improve the cutting performance in finish hard turning remains unexplored, and can be addressed in future studies.

Declaration of Competing Interest

The authors reported no declarations of interest.

Acknowledgements

This study was commissioned and fully funded by SECO Tools India (P) Ltd. All tools, tool holders and the hardened workpiece material used in this study were provided by SECO. The authors wish to thank Mr. Per Alm, Mr. Vijay Dole, Mr. Sudarshan Patil, and Mr. Gajanan Ugale from SECO Tools India (P) Ltd. for their technical inputs during these investigations. The authors also wish to thank Mr. Prateek Gupta, Mr. Mohit Sinha, and Mr. Pankaj Deora, students in the Department of Mechanical Engineering at the IIT Kanpur for their help in carrying out the preliminary experiments for this study.

References

[1] Poulachon G, Moisan A, Jawahir IS. Tool-wear mechanisms in hard turning with polycrystalline cubic boron nitride tools. Wear 2001;250–251:576–86. https://doi.org/10.1016/S0043-1648(01)00609-3.
[2] Barry J, Byrne G. The mechanisms of chip formation in machining hardened steels. J Manuf Sci Eng Trans ASME 2002;124:528–35. https://doi.org/10.1115/1.1455643.
[3] Chou YK, Evans CJ, Barash MM. Experimental investigation on cubic boron nitride turning of hardened AISI 52100 steel. J Mater Process Technol 2003;134:1–9. https://doi.org/10.1016/S0924-0136(02)00070-5.
[4] Sobiyi K, Sigalas I, Akdogan G, Turan Y. Performance of mixed ceramics and CBN tools during hard turning of martensitic stainless steel. Int J Adv Manuf Technol 2015;77:861–71. https://doi.org/10.1007/s00170-014-6506-z.
[5] Özel T, Karpat Y, Srivastava A. Hard turning with variable micro-geometry PcBN tools. CIRP Ann Manuf Technol 2008;57:73–6. https://doi.org/10.1016/j.cirp.2008.03.063.
[6] Yallese MA, Chaoui K, Zeghib N, Boulanouar L, Rigal JF. Hard machining of hardened bearing steel using cubic boron nitride tool. J Mater Process Technol 2009;209:1092–104. https://doi.org/10.1016/j.jmatprotec.2008.03.014.
[7] Sadik MI. Wear development and cutting forces on CBN cutting tool in Hard Part turning of different hardened steels. Procedia Cirp 2012;1:232–7. https://doi.org/10.1016/j.procir.2012.04.042.
[8] Bouacha K, Yallese MA, Khamel S, Belhadi S. Analysis and optimization of hard turning operation using cubic boron nitride tool. Int J Refract Met Hard Mater 2014;45:160–78. https://doi.org/10.1016/j.ijrmhm.2014.04.014.
[9] Huang Y, Liang SY. Cutting forces modeling considering the effect of tool thermal property—application to CBN hard turning. Int J Mach Tools Manuf 2003;43:307–15. https://doi.org/10.1016/S0890-6955(02)00185-2.
[10] Dogra M, Sharma VS, Sachdeva A, Suri NM, Dureja JS. Tool wear, chip formation and workpiece surface issues in CBN hard turning: a review. Int J Precis Eng Manuf Technol 2010;11:341–58. https://doi.org/10.1007/s12541-010-0040-1.
[11] Bartarya G, Choudhury SK. State of the art in hard turning. Int J Mach Tools Manuf 2012;53:1–14. https://doi.org/10.1016/j.ijmachtools.2011.08.019.
[12] Huang Y, Chou YK, Liang SY. CBN tool wear in hard turning: a survey on research progresses. Int J Adv Manuf Technol 2007;35:443–53. https://doi.org/10.1007/s00170-006-0737-6.
[13] Kawasegi N, Sugimori H, Morimoto H, Morita N, Hori I. Development of cutting tools with microscale and nanoscale textures to improve frictional behavior. Precis Eng 2009;33(3):248–54. https://doi.org/10.1016/j.precisioneng.2008.07.005.
[14] Olleak A, Özel T. 3D finite element modeling based investigations of micro-textured tool designs in machining titanium alloy Ti-6Al-4V. Procedia Manuf. 2017;10:536–45.
[15] Obikawa T, Kamio A, Takaoka H, Osada A. Micro-texture at the coated tool face for high performance cutting. Int J Mach Tools Manuf 2011;51(12):966–72. https://doi.org/10.1016/j.ijmachtools.2011.08.013.
[16] Sugihara T, Enomoto T. Improving anti-adhesion in aluminum alloy cutting by micro stripe texture. Precis Eng 2012;36(2):229–37. https://doi.org/10.1016/j.precisioneng.2011.10.002.
[17] Fatima A, Mativenga PT. Assessment of tool rake surface structure geometry for enhanced contact phenomena. Int J Adv Manuf Technol 2013;69(1):771–6. https://doi.org/10.1007/s00170-013-5079-6.
[18] Vasumathy D, Meena A. Influence of micro scale textured tools on tribological properties at tool-chip interface in turning AISI 316 austenitic stainless steel. Wear 2017;376:1747–58.
[19] Kümmel J, Braun D, Gibmeier J, Schneider J, Greiner C, Schulze V, et al. Study on micro texturing of uncoated cemented carbide cutting tools for wear improvement and built-up edge stabilisation. J Mater Process Technol 2015;215:62–70.
[20] Koshy P, Tovey J. Performance of electrical discharge textured cutting tools. CIRP Ann Manuf Technol 2011;60:153–6.
[21] Durairaj S, Guo J, Aramcharoen A, et al. An experimental study into the effect of micro-textures on the performance of cutting tool. Int J Adv Manuf Technol 2018;98:1011–30. https://doi.org/10.1007/s00170-018-2309-y.
[22] Qi Y, Nguyen V, Melkote S, Varenberg M. Wear of WC inserts textured by shot peening and electrical discharge machining. Wear 2020;452–453:203279. https://doi.org/10.1016/j.wear.2020.203279. ISSN 0043-1648.
[23] Fatima A, Mativenga PT. A comparative study on cutting performance of rake-flank face structured cutting tool in orthogonal cutting of AISI/SAE 4140. Int J Adv Manuf Technol 2015;78(9):2097–106. https://doi.org/10.1007/s00170-015-6799-6.
[24] Liu Y, Deng J, Wu F, Duan R, Zhang X, Hou Y. Wear resistance of carbide tools with textured flank-face in dry cutting of green alumina ceramics. Wear 2017;372:91–103.
[25] Sugihara T, Tanaka H, Enomoto T. Development of novel CBN cutting tool for high speed machining of inconel 718 focusing on coolant behaviors. Procedia Manuf 2017;10:436–42. https://doi.org/10.1016/j.promfg.2017.07.021.
[26] Sugihara T, Nishimoto Y, Enomoto T. Development of a novel cubic boron nitride cutting tool with a textured flank face for high-speed machining of Inconel 718. Precis Eng 2017;48:75–82. https://doi.org/10.1016/j.precisioneng.2016.11.007.
[27] Duan R, Deng J, Ai X, Liu Y, Chen H. Experimental assessment of derivative cutting of micro-textured tools in dry cutting of medium carbon steels. Int J Adv Manuf Technol 2017;92:3531–40. https://doi.org/10.1007/s00170-017-0360-8.
[28] Duan R, Deng J, Lei S, Ge D, Liu Y, Li X. Effect of derivative cutting on machining performance of micro textured tools. J Manuf Process 2019;45:544–56. https://doi.org/10.1016/j.jmapro.2019.07.037.
[29] Ranjan P, Hiremath SS. Role of textured tool in improving machining performance: a review. J Manuf Process 2019;43:47–73. https://doi.org/10.1016/j.jmapro.2019.04.011.
[30] Bruzzone AAG, Costa HL, Lonardo PM, Lucca DA. Advances in engineered surfaces for functional performance. CIRP Ann Manuf Technol 2008;57:750–69. https://doi.org/10.1016/j.cirp.2008.09.003.
[31] Sharma V, Pandey PM. Recent advances in turning with textured cutting tools: a review. J Clean Prod 2016;137:701–15. https://doi.org/10.1016/j.jclepro.2016.07.138.
[32] Arslan A, Masjuki HH, Kalam MA, Varman M, Mufti RA, Mosarof MH, et al. Surface texture manufacturing techniques and tribological effect of surface texturing on cutting tool performance: a review. Crit Rev Solid State Mater Sci 2016;41:447–81. https://doi.org/10.1080/10408436.2016.1186597.
[33] Gajrani KK, Ravi Sankar M. State of the art on micro to nano textured cutting tools. Mater Today Proc 2017;4:3776–85. https://doi.org/10.1016/j.matpr.2017.02.274.
[34] Kumar CS, Patel SK. Application of surface modification techniques during hard turning: present work and future prospects. Int J Refract Met Hard Mater 2018;76:112–27. https://doi.org/10.1016/j.ijrmhm.2018.06.003.
[35] Kang Z, Fu Y, Kim DM, Joe HE, Fu X, Gabor T, et al. From macro to micro, evolution of surface structures on cutting tools: a review. JMST Adv 2019;1:89–106. https://doi.org/10.1007/s42791-019-0009-x.
[36] Chen Y, Wang J, Chen M. Enhancing the machining performance by cutting tool surface modifications: a focused review. Mach Sci Technol 2019;23:477–509. https://doi.org/10.1080/10910344.2019.1575412.
[37] Arumugaprabu V, Ko TJ, Thirumalai Kumaran S, Kurniawan R, Uthayakumar M. A brief review on importance of surface texturing in materials to improve the

tribological performance. Rev Adv Mater Sci 2018;53:40–8. https://doi.org/10.1515/rams-2018-0003.
[38] Xing Y, Deng J, Zhao J, Zhang G, Zhang K. Cutting performance and wear mechanism of nanoscale and microscale textured Al2O3/TiC ceramic tools in dry cutting of hardened steel. Int J Refract Met Hard Mater 2014;43:46–58. https://doi.org/10.1016/j.ijrmhm.2013.10.019.
[39] Orra K, Choudhury SK. Tribological aspects of various geometrically shaped micro-textures on cutting insert to improve tool life in hard turning process. J Manuf Process 2018;31:502–13. https://doi.org/10.1016/j.jmapro.2017.12.005.
[40] Kim DM, Bajpai V, Kim BH, Park HW. Finite element modeling of hard turning process via a micro-textured tool. Int J Adv Manuf Technol 2015;78:1393–405. https://doi.org/10.1007/s00170-014-6747-x.
[41] Kim DM, Lee I, Kim SK, Kim BH, Park HW. Influence of a micropatterned insert on characteristics of the tool-workpiece interface in a hard turning process. J Mater Process Technol 2016;229:160–71. https://doi.org/10.1016/j.jmatprotec.2015.09.018.
[42] Schultheiss F, Fallqvist M, M'Saoubi R, Olsson M, Ståhl JE. Influence of the tool surface micro topography on the tribological characteristics in metal cutting-Part II Theoretical calculations of contact conditions. Wear 2013;298–299:23–31. https://doi.org/10.1016/j.wear.2012.11.067.
[43] https://www.secotools.com/article/66778?language=en, accessed on 9th March 2020.
[44] ISO. Tool-life testing with single-point turning tools. 3685. 1993.
[45] Sharma S, Mandal V, Ramakrishna SA, Ramkumar J. Numerical simulation of melt hydrodynamics induced hole blockage in Quasi-CW fiber laser micro-drilling of TiAl6V4. J Mater Process Technol 2018 Dec;1(262):131–48.
[46] Tseng AA. Recent developments in micromilling using focused ion beam technology. J Micromechanics Microengineering 2004;14(4).
[47] CUTPRO V11.2. Adv. Mach. Simul. Softw. ©MAL Inc n.d.
[48] Shaw MC, Vyas A. The mechanism of chip formation with hard turning steel. CIRP Ann Manuf Technol 1998;47(1):77–82. https://doi.org/10.1016/S0007-8506(07)62789-9. ISSN 0007-8506.
[49] Kountanya R, Al-Zkeri I, Altan T. Effect of tool edge geometry and cutting conditions on experimental and simulated chip morphology in orthogonal hard turning of 100Cr6 steel. J Mater Process Technol 2009;209(11):5068–76. https://doi.org/10.1016/j.jmatprotec.2009.02.011. ISSN 0924-0136.
[50] Chen T, Guo J, Wang D, et al. Experimental study on high-speed hard cutting by PCBN tools with variable chamfered edge. Int J Adv Manuf Technol 2018:4209–16. https://doi.org/10.1007/s00170-018-2276-3.
[51] Neslušan M, Urík J, Mičietová A, Minárik P, Píška M, Čilliková M. Decomposition of cutting forces with respect to chip segmentation and white layer thickness when hard turning 100Cr6. J Manuf Process 2020;50:475–84. https://doi.org/10.1016/j.jmapro.2020.01.004. ISSN 1526-6125.
[52] Nakayama K, Arai M, Kanda T. Machining characteristics of hard materials. CIRP Ann Manuf Technol 1988;37-1:89–92. https://doi.org/10.1016/S0007-8506(07)61592-3.
[53] Grzesik W. Influence of tool wear on surface roughness in hard turning using differently shaped ceramic tools. Wear 2008;265(3–4):327–35. https://doi.org/10.1016/j.wear.2007.11.001.
[54] Bäker M. Finite element simulation of high-speed cutting forces. J Mater Process Technol 2006;176(1–3):117–26. https://doi.org/10.1016/j.jmatprotec.2006.02.019. ISSN 0924-0136.
[55] Sun S, Brandt M, Dargusch MS. Characteristics of cutting forces and chip formation in machining of titanium alloys. Int J Mach Tools Manuf 2009;49(7–8):561–8. https://doi.org/10.1016/j.ijmachtools.2009.02.008. ISSN 0890-6955.